



ORIGINAL ARTICLE

Lichen planus drugs re-purposing as potential anti COVID-19 therapeutics through molecular docking and molecular dynamics simulation approach

Unnati Soni¹, Pratyush Singh², Om Prakash Gupta³, Shalini Gupta^{4*}, Saurabh Pratap Singh⁴, Prerna Singh⁴, Sangeeta Singh¹, Krishna Mishra¹

¹Department of Applied Sciences, Indian Institute of Information Technology, Allahabad, Uttar Pradesh, India, ²Department of Oral Pathology and Microbiology, Maharana Pratap Dental College, Kanpur, Uttar Pradesh, India, ³Department of General Surgery, Career Institute of Medical Sciences, Lucknow, Uttar Pradesh, India, ⁴Department of Oral Pathology and Microbiology, King George's Medical University, Lucknow, Uttar Pradesh, India

ARTICLE INFO

Article history:

Received: August 27, 2021

Revised: October 03, 2022

Accepted: January 08, 2022

Published online: March 01, 2022

Keywords:

angiotensin converting enzyme-2
main-protease
spike glycoprotein
oral lichen planus
SARS-CoV-2

*Corresponding author:

Shalini Gupta
Department of Oral Pathology and
Microbiology, King George's Medical
University, Lucknow,
Uttar Pradesh - 226 003, India.
Email: sgmds2002@yahoo.co.in

ABSTRACT

Background and Aim: The present study intends to investigate COVID-19 by targeting their main proteins with 17 selected drugs used for treating Oral Lichen Planus (OLP) which is a chronic mucocutaneous disorder. Here, an attempt is made to gain better insight into the structure of various drugs targeting specific proteins which will be helpful in developing drugs useful for therapeutic and preventive measures.

Method: *In silico* studies, molecular docking and molecular dynamic simulations were performed to repurpose the therapeutic drugs (n = 17) which were used to treat OLP against COVID-19. In addition, the maximum binding affinities of the key protein spike glycoprotein, main-protease (M^{pro}) of coronavirus, and Angiotensin-Converting Enzyme-2 (ACE-2) in the human body were evaluated with the selected drugs.

Results: Epigallocatechin-3-gallate (EGCG) showed the highest docking values among the drugs selected for repurposing. Among the target proteins, EGCG has shown maximum binding affinity with ACE-2 receptor. Further, according to the molecular dynamic simulation studies, EGCG has shown the least conformational fluctuations with M^{pro}.

Conclusion: EGCG can be a potential inhibitor drug which can bind with ACE-2 receptor thus inhibiting the interaction of mainly M^{pro} protein and spike glycoprotein of SARS-CoV-2.

Relevance for Patients: EGCG, a natural compound shows antiviral potential having considerably high affinity and stability with SARS-CoV-2. It might be further employed as a lead drug against selective inhibitors of SARS-CoV-2 for the therapeutic management of COVID-19 patients after necessary clinical trials.

© 2022 Author(s). This is an Open

Access article distributed under the terms

of the Creative Commons Attribution-

NonCommercial License, permitting all non-

commercial use, distribution, and reproduction

in any medium, provided the original work is

properly cited.

1. Introduction

The recent worldwide unprecedented outbreak of the novel COVID-19 has taken a toll on the medical and dental practitioners all across the globe. According to recent statistics, covid-19 infected person have already crossed 219 million cases worldwide of which causing death of 45.5 million people [1]. The devastating impact has raised alarms across the globe, especially in the developing world like ours where healthcare amenities are vulnerable. Medical personals all over the world are doing their utmost effort to prevent and control disease outbreaks caused by corona virus, which was originally documented in Wuhan city, China on 12th December 2019. The World Health Organization (WHO) on 11th February 2020 officially announced current pandemic disease to be named COVID-19 is caused by Severe Acute Respiratory Syndrome Coronavirus 2 (SARS-CoV-2). COVID-19 belongs

to the *Coronaviridae* family (subfamily *Coronavirinae*), of which infected members producing early signs and symptoms ranging from the common cold, sore throat to severe pneumonia leading to ultimately death [2]. During this period to control COVID-19 various measures have emerged to detect, diagnose and prevent the spread of this disease, however, still, no successful therapies have been developed. But still few drugs have shown some results in COVID-19 patients such as lopinavir, ritonavir, antiviral, chloroquine and hydroxychloroquine, convalescent plasma, and stem cell therapy. Hence, to prevent the spread of SARS-CoV-2 there is a developing need to determine potential therapeutic agents [2,3]. In ongoing research, many attempts are being made by utilizing advanced complex computational approaches which may lead to screening large chemical libraries. For the rapid development of successful potential therapeutic drugs, screening test and clinical trial methods alone may not be enough. Computational biology which includes part of bioinformatics is also an important tool which is used to develop algorithms, based on the collection and analysis of biological data such as molecular docking (MD)-based virtual high-throughput screening (vHTS) thus helping us designing drugs based on their chemical structure to find potential lead drugs among various chemical libraries [2].

The genetic sequencing of SARS-CoV-2 encodes several proteins such as the Main protease (M^{pro} or $3CL^{pro}$), Spike glycoprotein S1 subunit which plays an important role in its pathophysiology and Human Angiotensin-converting enzyme-2 (ACE-2) receptor in the human body which acts entry point for virus are the main part of our study [3]. Thus, the main target of our study is to find a lead drug that can counteract these encoded proteins and inhibit its interaction with ACE-2 receptor.

1.2. Interaction and their effect between Lichen Planus and COVID-19

Oral lichen planus (OLP) is a chronic inflammatory autoimmune disease [4]. It is mostly CD8+T-cell mediated autoimmune response whose pathogenesis includes the movement of lymphocytes into the epithelium thus encountering specific antigen, T-cell lymphocyte initiation, proliferation as well as the killing of keratinocyte. It also includes the basement membrane disruption, the release of mast cell, chemokines, and matrix metalloproteinase (MMP) activation mainly MMP-2 and MMP-9 [4,5]. ACE-2, shares some homology of ACE, can offset the negative role of the renin-angiotensin system in many diseases and also it is widely expressed in various human organs and tissues, has extensive biological activities [6-8]. Hence, the presence of ACE-2 at various locations will act as a target site, usually the oral cavity as per report which is mainly considered as a potential site through which COVID-19 virus enters and acts immediately [6].

SARS-CoV-2 spike glycoprotein present in the virus contains receptor-binding region, which attaches with ACE-2 receptors present on the cell surfaces in host cell leading to its loss of function. This factor is most important as all the research strategies are targeting this area to develop potential drugs, antibodies, or vaccines [7,8]. M^{pro} (M^{pro} or $3CL^{pro}$) breaks down spike protein

into subunits and helps virus to mature and replicate in host cell. Normally ACE-2 degrades Angiotensin II to heptapeptide vasodilatory Ang 1-7 which, in turn, maintains balance between ACE and ACE-2 thus regulating Angiotensin II levels. However, this function becomes impaired due to loss of function of ACE-2 following binding by SARS-CoV-2 which leads to uncontrolled Angiotensin II level [6,8]. Studies have shown in OLP there is the presence of 60% degranulated mast cells as compared to 20% in normal buccal mucosa. Activation of degranulated mast cell occurs following interaction with CD8+ cytotoxic cells upon which proinflammatory mediators such as Tumor Necrosis factor α (TNF- α), chymase, and tryptase are released which, in turn, activates T cells which further secrete regulated on activation, normal T cell expressed and secreted (RANTES). Thus, RANTES attracts CCR + mast cells and inflammatory cells into the epithelium, triggering further mast cell degranulation leading it into a vicious cycle. Chymase which originates from mast cells, endothelial and mesenchymal cells helps in the regulation of angiotensin II level [6,8]. We hypothesized that due to increased mast cell degranulation, a large amount of chymase is released which further cleaves angiotensin I to generate angiotensin II resulting in increased ACE-2 but due to virus binding to its receptor it loses its function leading to imbalance [6,7]. Thus further affecting the expression of MMPs mainly MMP-2 and MMP-9 via ACE-2-Ang1-7-Mas axis and ERK1/2 signaling pathway [9,10].

Effects of Angiotensin II comprises proinflammatory, proliferative, and pro-fibrotic activities which are non-hemodynamic in nature. Angiotensin II also act as inflammatory mediator in tissues such as the kidney, heart, and vasculature by promoting the expression of cytokines such as IL-6, IL-12, IL-12 [8-10]. Further, Angiotensin II leads to the formation of Angiotensin type 1 receptor (AT_1R) and Angiotensin type 2 receptor (AT_2R) which regulates dendritic cells in migration. These receptors also act on T-cells leading to their activation, proliferation, and release of Chemokines/cytokines [10] which further aggravates OLP and COVID-19 condition.

Drugs like Hydrochloroquine and many others are used in clinical trial studies to treat covid-19. These few drugs are also frequently used to treat OLP, therefore we hypothesized that there must be few similar proteins that are targeted by these drugs found in OLP and Covid-19. After employing an extensive MD-based vHTS, we identified the 17 potential compounds from the database for the present study that have been investigated in recent years because of their various pharmacological properties and immunomodulatory activities used in the treatment of OLP disease. Drugs such as Prednisone, Dapsone, Fluocinonide, Curcumin, Epigallocatechin-3-gallate (EGCG), Fenretinide, Phenytoin, Hydroxy-chloroquine etc which act as anti-inflammatory, antineoplastic, antifungal, antioxidant, and immunosuppressive [3]. Our hypothesis is these selected drugs may inhibit or suppress by targeting various proteins responsible for COVID-19 and OLP, thus providing us with a natural and inexpensive therapeutic strategy. Also if OLP patient is affected with COVID-19, these drugs may bridge the gap between these

two entities and provide us with a solution which we were lacking before.

2. Materials and Method

2.1. Ligand retrieval and preparation

The structures of drugs that are proposed to be repurposed as therapeutic drugs against COVID-19, generally used against chronic inflammatory disease OLP, were selected through a literature survey. For this study, Remdesivir and Ivermectin have been selected as reference antiviral. Three-dimensional conformers of the compounds were downloaded from the PubChem database. By adopting Optimized Potentials for Liquid Simulations-3 (OPLS3) in the Ligprep module of Schrödinger [11], structures were converted into efficient, accurate, and energy minimized 3D molecular models.

2.2. Selection and preparation of target protein

The three-dimensional structure of drug targets M^{pro} (PDB ID: 6LU7) and S1 subunit of spike glycoprotein of SARS-CoV-2 (PDB ID: 6VYB) and their receptor in the human body, *i.e.*, human ACE-2 (PDB ID: 1R42) were retrieved from the RCSB Protein Data Bank. The protein structures were processed through Protein Preparation Wizard [12], Maestro suite of Schrödinger, in three steps *i.e.* pre-processing to delete unwanted chains and water molecules, assigning bond orders, and adding hydrogen atoms. Then optimizing the molecule and lastly, OPLS3 force field was utilized for controlled minimization of protein structure. The Receptor Grid Generation of Glide module of Schrödinger was used for grid file generation [13]. Predicted active sites from the literatures were used for receptor grid generation, the spike protein active site consists of amino acid residues LYS417, GLY446, TYR449, ASN487, GLN493, GLY496, THR500, and GLY502. Similarly, the active site of Human ACE2 protein includes ASP30, GLN42, ASP38, GLN24, TYR83, GLU35, LYS353, TYR41, and LYS353 [14]. While, interacting amino acid residues of the enzyme M^{pro} includes LYS5, THR25, GLN10, LYS137, LEU141, ANS142, GLY143, SER144, CYS145, TYR154, HIS164, MET165, GLU166, GLN189, ASP197, ANS238, ILE249, GLU288, ASP289, GLU290, PRO293, PHE294, VAL 297, and ARG298 [15,16].

2.3. MD

Maestro 12.4 (Schrodinger 2020–2) was used for the MD of selected OLP drugs with M^{pro}, spike glycoprotein, and human ACE-2. After protein and ligand preparation, receptor grids generated using active amino acid residues and further used for protein-ligand docking. Ligand-Docking function of Maestro suite was used with extra precision (XP) to perform the docking and calculation of various docking parameters. The ligands were retained flexible while the proteins were considered rigid applying Epik state penalties. At last, the pose viewer file was used as output of process for calculation. PyMol 2.4.0 was used for visualization, editing, and generation of 3D structures of merged protein-ligand complex.

2.4. Molecular dynamic simulation (MDS)

MDS study of docked complexes was performed using Groningen Machine for Chemical Simulations (GROMACS 2019.6) package with the standard CHARMM36 all-atom force field (Huang and MacKerell, 2013). The three protein-ligand complexes were selected for their conformational and stability analysis. PRODRG server was used to generate topology files of ligand file (Schüttelkopf and Van Aalten, 2004). For solvation of complex, TIP3P water model in a dodecahedron box with boundaries 1.2 nm was opted. Counter ions (NaCl) were added to the complex in order to neutralize the system charge. In order to minimize system energy, the steepest descent algorithm without constraints was run for 5000 steps [17]. Equilibration of five complexes was done under NVT and NPT conditions for a period of 5000 ps with 300K temperature and coupling constant $\tau_t = 0.1$ ps. The Berendsen weak-coupling method was used for maintaining the temperature and pressure of the system. To constrain the bond length of heavy atoms, Linear Constraint Solver (LINCS) algorithm was used [18]. Finally, a 50 ns production run was performed for each system. Van der Waals interactions were maintained using the Lennard-Jones potential, and the particle-mesh Ewald-method was used for the electrostatic interactions [19]. For the entire simulation time, every 2ps final coordinate trajectories were saved. GROMACS modules such as `gmx_rmsd`, `gmx_rmsf`, and `gmx_gyratio` were used to analyze the MD trajectories. Further, QTGrace tool was utilized for the interpretation of MD results QtGrace download | SourceForge.net,” n.d.).

2.5. Prediction of binding energies via MMGBSA

To improve the validation in docking studies, we employed Prime-MMGBSA (molecular mechanics energies joint with the generalized Born and surface area continuum solvation) of the Maestro to estimate relative binding energies for the list of ligands (reported in kcal/mol). The calculated binding energies are estimated free energies of binding; thus a more negative value shows stronger binding of a ligand with the protein. Binding energy is calculated based on the following equation,

$$\text{MMGBSA } dG_{\text{Bind}} = dG_{\text{(Complex)}} - \{dG_{\text{(Receptor)}} + dG_{\text{(Ligand)}}\}$$

3. Results

3.1. Ligand retrieval and preparation

A total of 17 drugs were selected on the basis of literature survey which is being used in the treatment of OLP. The details of the selected drugs along with their PubChem IDs and pharmacological properties are given in table 1. Their structures are given in supplementary data (Table 1).

3.2. Selection and preparation of target protein

The protein structures selected for the docking studies are shown in Figures 1-3 for spike protein, ACE-2, and M^{pro} respectively given in the supplementary data. A grid box was

Table 1. List of drugs used against OLP with their structures and pharmacological properties.

No.	Drugs used against OLP	PubChem ID	Pharmacological properties
1.	Hydroxy-chloroquine	3652	Immunosuppressive, antiautophagy, and antimalarial
2.	Prednisone	5865	Anti-inflammatory and immunomodulating
3.	Dapsone	2955	Anti-inflammatory and anti-bacterial
4.	Flucanide	9642	Anti-inflammatory and antipruritic
5.	Curcumin	969516	Anti-inflammatory, antineoplastic and antifungal
6.	Azathioprine	2265	Cytotoxic and immunosuppressive
7.	Epigallocatechin-3-gallate	65064	Antioxidant
8.	Triamcinolone acetonide	6436	Immunosuppressive and anti-inflammatory
9.	Phenytoin	1775	Non-sedative antiepileptic agent with anticonvulsant activity
10.	Griseofulvin	441140	Fungistatic agent
11.	Trioxsalen	5585	Photosensitizing agent and a dermatologic drug
13.	Tacrolimus	445643	Immunosuppressive
14.	Clobetasol propionate	32798	Anti-inflammatory, anti-pruritic, and vasoconstrictive
15.	Levamisole	26879	Antinematodal, antirheumatic, immunomodulator, and immunological adjuvant
16.	Fenretinide	5288209	Antineoplastic and chemopreventive
17.	Isotretinoin	5282379	Antineoplastic, keratolytic drug and a teratogenic agent
Reference antivirals			
1.	Remdesivir	121304016	Antiviral drug, a prodrug and an anticoronaviral agent
2.	Ivermectin	6321424	Antiparasitic, anti-viral, anti-infective

generated that identifies the centroid of the dynamic site which is available for docking. The produced grid determines the positioning of protein by the exclusion of ligands which might be present already and hence finalize the location and extent of the active site that has been anticipated. The grid coordinates of the receptor for (x, y, and z) axis was as follows in Table 2:

3.3. MD

The results obtained through the Glide module for the docking of protein structure for Spike, ACE-2, and Mpro with the selected drugs used in OLP treatment were based on the docking score as well as the glide energy of the ligand-receptor complex is portrayed in Table 3. EGCG shows the more negative binding energy against all the selected target protein, i.e., Spike (−5.169), ACE-2 (−5.583), and M-pro (−5.020), which means having highest binding affinity towards them. Further, the Curcumin (−4.746) and Fenretinide (−4.417) were also found to be having higher binding affinity toward Spike protein but not for ACE-2 and Mpro. The other selected drugs are not turned out to be effective as the docking scores are quite low. Among all Levamisole showed the lowest docking score of −1.627, −1.757 for Spike and ACE-2, respectively. While for Mpro protein Fenretinide showed the lowest docking score, i.e., −1.364.

The docking results of the drug EGCG against SARS CoV-2 target proteins are found to be encouraging thus they can be suggested to be repurposed as therapeutic drug against COVID-19.

The docking results of the drug Epigallocatechin 3-gallate are found to be highest against all three target proteins of SARS

Table 2. Proteins and grid box centers for molecular docking.

Protein	Center		
	x	y	z
Spike glycoprotein	233.73	184.06	275.44
Human ACE2	78.79	76.84	32.52
Main protease	−23.57	11.16	57.84

CoV-2 (detailed docking result is given in table 4), thus it can be suggested to be repurposed as therapeutic drug against COVID-19. In addition, interaction images displaying well-versed interaction of amino acids of these proteins i.e. spike protein, human ACE-2 and Mpro have been shown in Figures 1-3 respectively along with the drug EGCG. Also, along with EGCG, Curcumin, Fenretide, and Prednisone have also shown promising interaction with target proteins and have considerable docking values; their binding interaction diagrams have been included in the supplementary data.

The docking scores of EGCG are found to be encouraging against all three selected targets. In table 5, the comparison among docking scores of predicted drug with standard or reference drugs has been shown. From the docking results, it can be observed that the reference antiviral remdesivir has shown better binding with spike proteins and has been found clinically effective against target proteins; however, with the increasing applications; adverse effects of remdesivir have been detected and become a concern of clinicians, while ivermectin has not shown any interaction with spike protein. Our predicted drug EGCG has also shown comparatively promising results against all target proteins and enzyme.

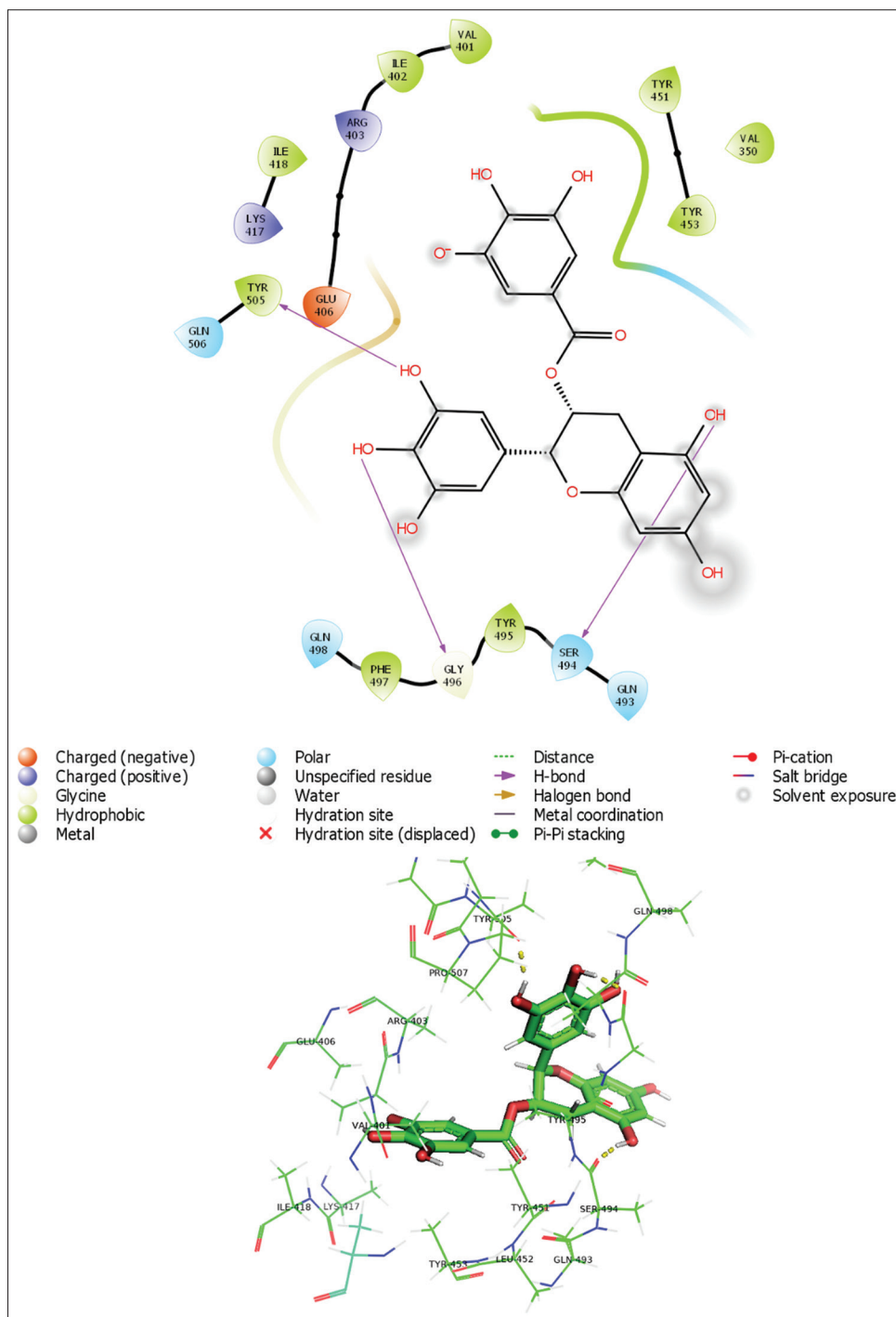


Figure 1. Interaction image of spike glycoprotein with Epigallocatechin-3-gallate.

3.4. MDS

RMSD and RMSF trajectories of all three complexes i.e. EGCG with 1R42, 6LU7, and 6VYB were analyzed (Figure 4). For 1R42-EGCG complex, RMSD value was observed with small deviations till the first 15 ns. Afterwards, continuous increase and decrease was observed till 26 ns, then found to be almost stable till 35 ns. Till 38ns again huge deviations were

observed, later till 45 ns decreased a little and again increased towards the end of 50 ns. In the case of 6LU7-EGCG complex, the RMSD value was stable till 28ns, then till 35 ns increased and again decreased and remained stable till 43 ns. After that, it fluctuated constantly till 47ns; again decreased and remained stable till the end of 50 ns. For 6VYB-EGCG complex, RMSD value was observed to be gradually increasing till 32 ns, decreased gradually for 45 ns, and again increased toward

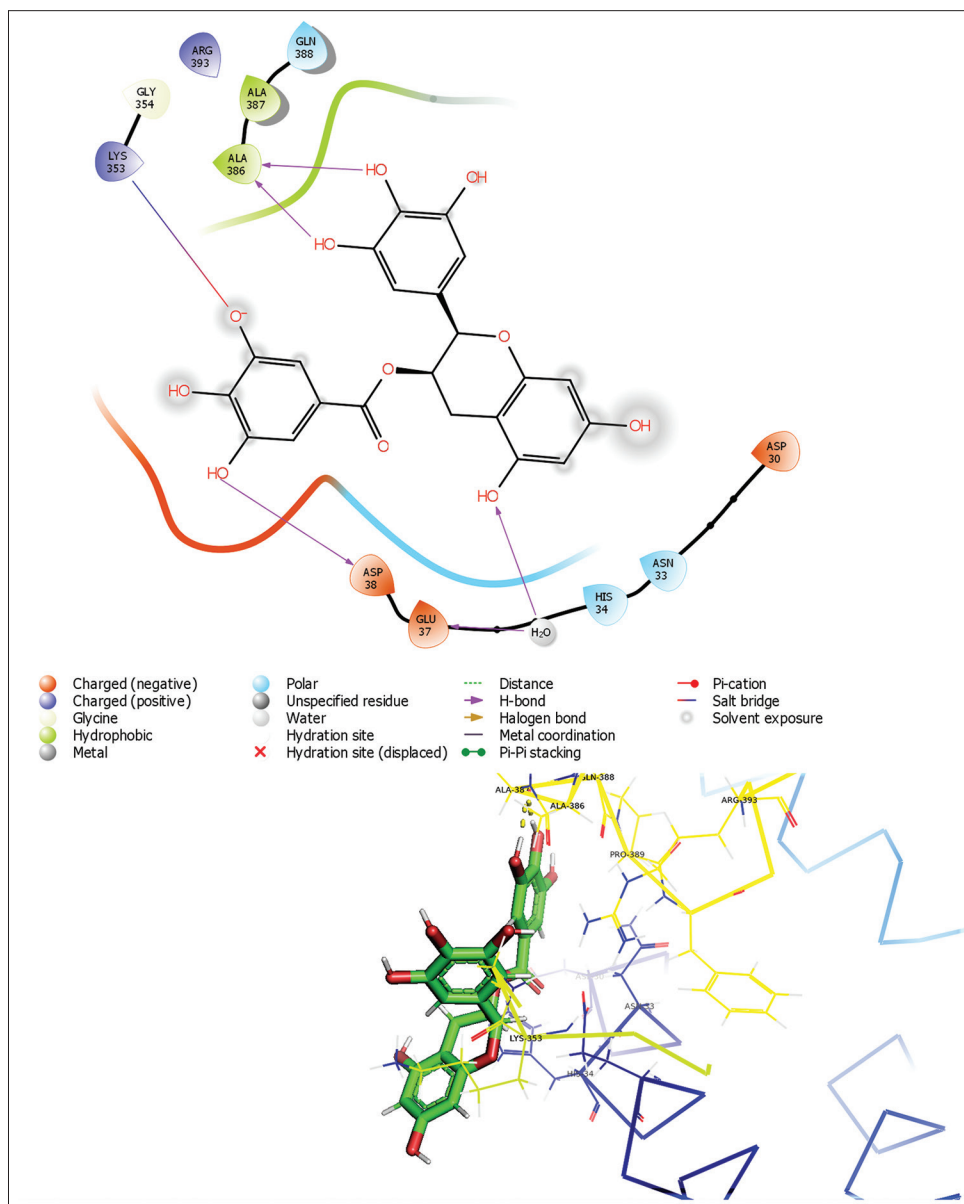


Figure 2. Interaction image of Human ACE-2 with Epigallocatechin-3-gallate.

the end of the 50 ns. Average RMSD values of 1R42-EGCG, 6LU7-EGCG, and 6VYB-EGCG complexes were found to be approximately 0.74 nm, 0.5 nm, and 2.25nm. From the RMSD plot it was observed that 6LU7-EGCG complex showed least deviations and remained more stable in comparison to 1R42-EGCG and 6VYB-EGCG complexes.

Further, the RMSF graphs of three complexes were analyzed to find out the behavior of residues (Figure 5). The average root mean square fluctuations of 1R42-EGCG, 6LU7-EGCG and 6VYB-EGCG complexes were observed to be 0.14 nm, 0.10 nm, and 1.2 nm, respectively. The graphs clearly depicted that 6LU7-EGCG complex had least conformational fluctuations in comparison to 1R42-EGCG and 6VYB-EGCG complexes.

Post-simulation binding mode of EGCG with all selected targets is given in Figures 6-8 with Spike protein, human ACE-2, and Mpro, respectively.

3.5. Prediction of binding energies via MMGBSA

Regarding further validation of the docking results, MMGBSA analysis has been performed for the evaluation of the relative binding energies of ligands with respective proteins and enzyme and its binding affinities have been compared with reference drug found effective against COVID-19, in terms of MMGBSA dG bind. In the results, significant binding affinities can be seen for EGCG comparative to remdesivir and ivermectin against all the three selected proteins. Result of MMGBSA studies of all other ligand is given in Table 6.

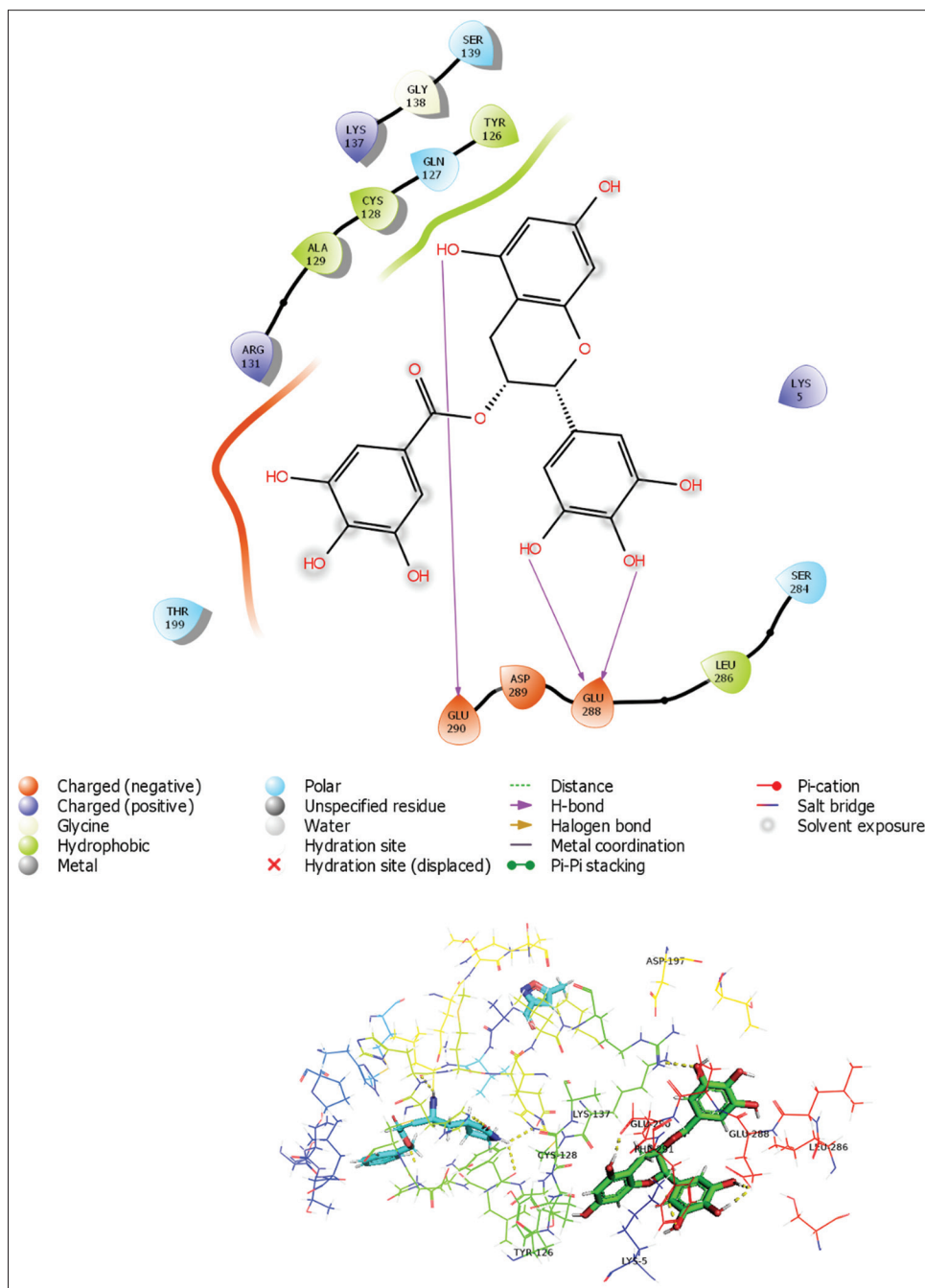


Figure 3. Interaction image of main-protease with Epigallocatechin-3-gallate.

Detailed result of MMGBSA studies of EGCG is given in [table 7](#).

Binding affinity of EGCG has been compared with remdesivir and ivermectin and found to be considerable against target proteins and enzyme with special reference to the spike protein; details are given in [table 8](#).

Furthermore, to compare the ability of the tested compound to bind with the mutations of the pocket residues of the spike protein, we have performed MD of selected OLP drugs with the various variants of spike protein such as alpha, beta, gamma, delta, and

omicron. We have observed satisfactory results with all above mentioned mutations of spike protein; their results have been added in supplementary data.

4. Discussion

SARS-CoV-2 is an enveloped positive single-stranded RNA *Betacoronavirus*, which belongs to family *Coronaviridae* which has caused the epidemic in humans globally. There are no officially approved antiviral drugs still available which could treat COVID-19 disease. Therefore, in major countries, more

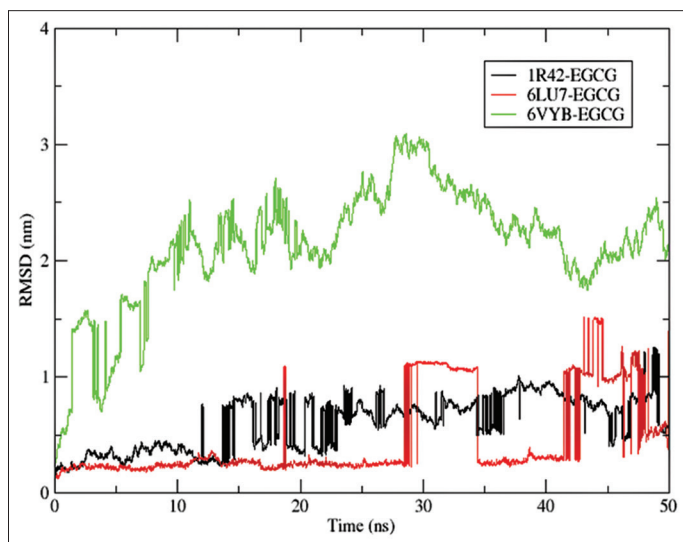


Figure 4. RMSD analysis of MD simulation trajectory of EGCG with 1R42, 6LU7, and 6VYB in 50 ns simulation time.

than 80 clinical trials are ongoing to identify any drugs such as chloroquine, remdesivir, favipiravir, lopinavir, ritonavir, and hydroxychloroquine which may be suitable in treating this disease [20,21]. However, the major disadvantages are that they have lots of side effects such as visual impairment, heart failure, seizures, hypokalemia, heart arrhythmias and ventricular tachycardia, and fibrillation [20]. Therefore, due to the major side effects present in these chemical drugs, natural products are gaining attention because they are much safer, cheaper, non-toxic, and more efficient for the treatment of COVID-19 [21,22]. The main objective of the researchers is to develop therapeutic antiviral drugs having broad-spectrum properties, thus by directly targeting the SARS-CoV-2 spike glycoprotein and ACE-2 receptor which are responsible for COVID-19 [22]. The best method to study mechanism of action of potential drugs is to study its chemical structure. A structural study on the coronavirus M^{pro} 3CL^{pro}, spike glycoprotein, and ACE-2 inhibitor complex established designing of drug against the coronavirus and demonstrated that these drug form high affinity to the target [23,24].

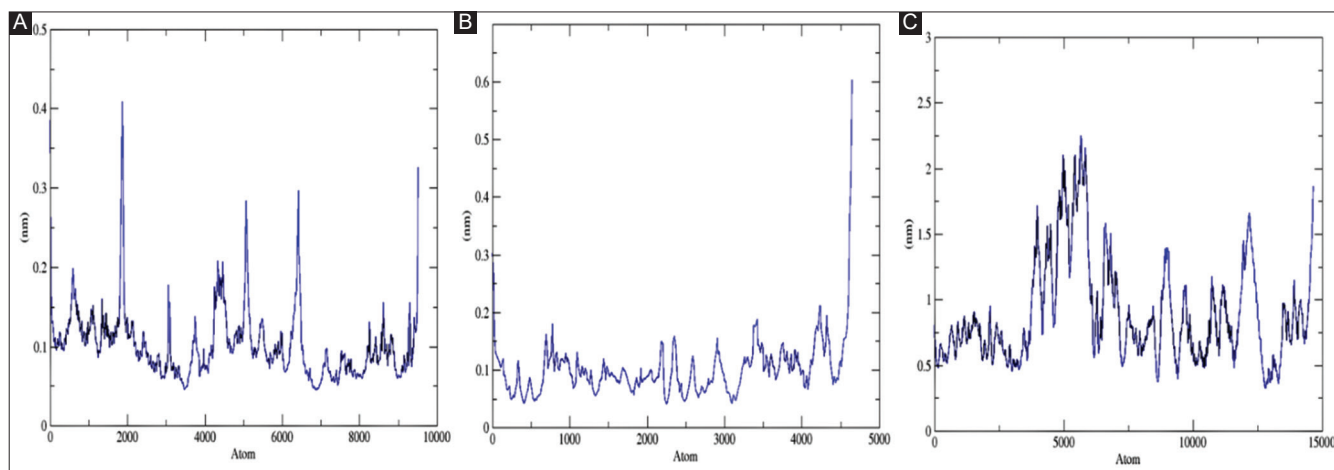


Figure 5. RMSF analysis of (A) EGCG-1R42 complex, (B) EGCG-6LU7 complex, and (C) EGCG-6VYB complex in 50 ns simulation time.

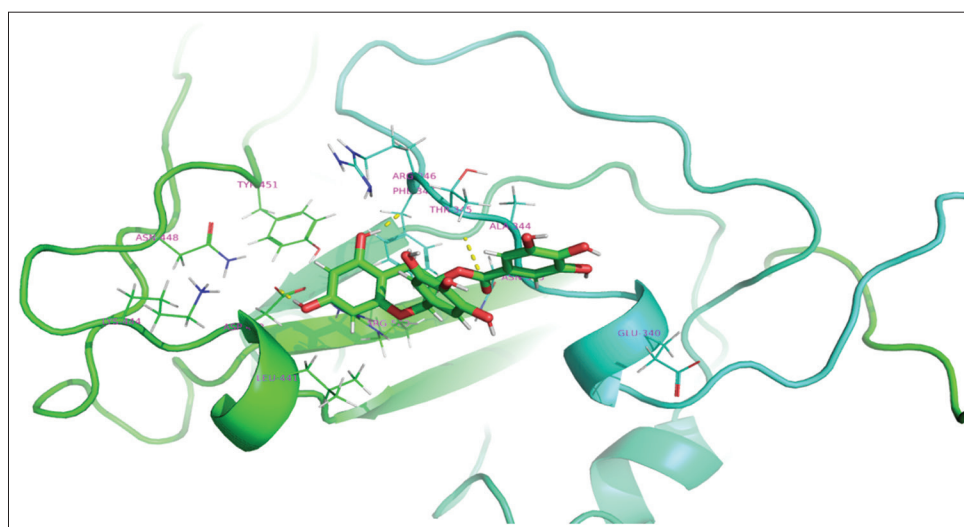


Figure 6. Post- MDS binding mode of EGCG with Spike protein.

Table 3. Molecular docking results of screened drugs with all three target proteins.

No.	Drugs used against OLP	Docking score		
		Spike glycoprotein (PDB ID: 6VYB)	ACE-2 (PDB ID: 1R42)	Main-protease (PDB ID: 6LU7)
1.	Epigallocatechin-3-gallate	-5.169	-5.583	-5.020
2.	Curcumin	-4.746	-2.982	-2.949
3.	Fenretinide	-4.417	-2.064	-1.364
4.	Phenytoin	-3.496	-2.803	-2.234
5.	Dapsone	-3.419	-2.957	-3.594
6.	Hydroxy-chloroquine	-3.416	-3.732	-2.609
7.	Prednisone	-3.322	-3.474	-4.439
8.	Trioxsalen	-2.952	-2.626	-2.174
9.	Griseofulvin	-2.943	-	-2.184
10.	Isotretinoin	-2.689	-2.273	-0.354
11.	Flucanide	-2.683	-2.490	-3.167
12.	Clobetasol propionate	-2.576	-	-1.842
13.	Triamcinolone acetonide	-2.565	-	-2.33
14.	Azathioprine	-2.390	-2.730	-2.785
15.	Levamisole	-1.627	-1.757	-1.780
16.	Tacrolimus	-	-	-2.158

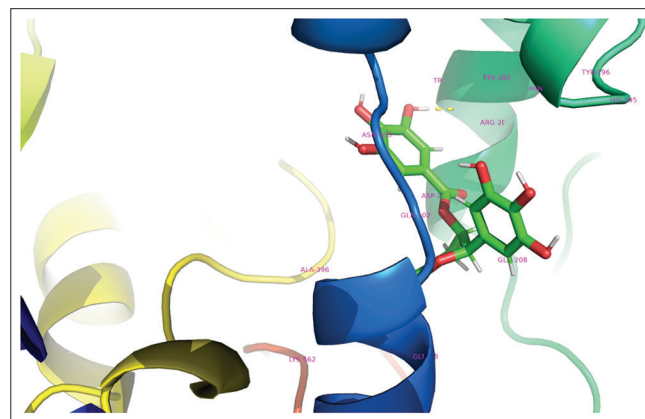
Table 4. Molecular docking results Epigallocatechin-3-gallate of with target protein.

Target protein	Docking score	Glide gscore	Glide emodel	Glide energy	Interacting amino acid	Interaction type
SARS-CoV-2 Spike Protein S1 Subunit (PDB ID: 6VYB)	-5.169	-5.248	-54.697	-45.585	SER 494, GLY 496, TYR 505	3 H-Bonds
Human Angiotensin-converting enzyme 2-ACE2 (PDB ID: 1R42)	-5.583	-5.661	-50.564	-44.632	ASP 38, GLU 37, LYS 353, ALA 386	4 H-Bonds, 1Salt bridge
SARS-CoV-2 Main Protease-M Pro/3CL (PDB ID: 6LU7)	-5.020	-6.869	-50.680	-40.942	GLU 288, GLU 290	3 H-bonds

Table 5. Comparison of docking scores of EGCG with reference drugs.

Target	Ligand		
	EGCG	Remdesivir	Ivermectin
ACE2	-5.583	-3.682	-3.462
Mpro	-5.020	-4.327	-2.813
Spike	-5.169	-7.120	-

For MD studies, the drugs were taken, which are commonly used for treating chronic muco-cutaneous disorder OLP, mentioned in Table.1. Our docking results confirmed that EGCG is the best drugs followed by Prednisone among the selected showing an inhibitory effect for M^{pro} (M^{pro} or 3CL^{pro}), spike glycoprotein, and ACE-2 in COVID-19. It was followed by Circumin and Fenentinide which are mainly effective against spike glycoprotein. Among all ligands, it is found that EGCG has attained the maximum docking score with all three significant proteins of SARS CoV-2. By comparing the result of docking of EGCG with all three target proteins, it is found that the proposed drug binds with ACE-2 more firmly having a better docking score (-5.583) than the other two proteins (spike glycoprotein: -5.169; M^{pro}: -5.020). Thus, it can be concluded that by inhibiting ACE-2, EGCG can prevent binding of ACE-2 with spike glycoprotein and

**Figure 7.** Post- MDS binding mode of EGCG with human ACE-2.

M^{pro} of SARS CoV-2; the chain A of 1R42 (ACE-2) was extracted to perform MD with EGCG, docking studies revealed that EGCG binds to residues ALA 387 of ACE-2 by forming two H-bonds. The MD simulation study of three complexes clearly showed that EGCG could be a potential inhibitor for 6LU7.

Epigallocatechin Gallate (EGCG) is found in plants such as green and black tea and act as phenolic antioxidant. EGCG also prevents oxidative stress which causes damage to cells. It can



Figure 8. Post- MDS binding mode of EGCG with Mpro.

Table 6. MMGBSA results of screened drugs with all three target proteins.

No.	Drugs used against OLP	MMGBSA dG Bind		
		Spike glycoprotein (PDB ID: 6VYB)	ACE-2 (PDB ID: 1R42)	Main-protease (PDB ID: 6LU7)
1.	Epigallocatechin-3-gallate	-52.14	-28.84	-36.96
2.	Curcumin	-62.27	-27.62	-25.77
3.	Fenretinide	-76.52	-48.78	-27.92
4.	Phenytoin	-35.29	-2.803	-18.97
5.	Dapsone	-35.44	-24.51	-27.78
6.	Hydroxy-chloroquine	-61.41	-44.40	-27.12
7.	Prednisone	-46.64	-28.56	-47.22
8.	Trioxsalen	-41.93	-29.84	-29.88
9.	Griseofulvin	-48.68	-	-25.51
10.	Isotretinoin	-51.56	-33.98	-3.60
11.	Flucanionide	-53.02	-19.16	-30.58
12.	Clobetasol propionate	-55.09	-	-26.44
13.	Triamcinolone acetonide	-47.63	-	-29.68
14.	Azathioprine	-31.72	-21.45	-15.64
15.	Levamisole	-40.72	-27.19	-29.31
16.	Tacrolimus	-	-	-28.73

Table 7. MMGBSA results of Epigallocatechin-3-gallate with target protein.

Target	MMGBSA dG Bind	MMGBSA dG Bind Coulomb	Ligand energy	Ligand Coulomb	Complex energy	Complex Coulomb	Receptor energy	Receptor Coulomb
Spike protein	-52.14	-26.28	-65.247	-67.201	-37342.252	-28691.669	-37224.868	-28598.186
ACE-2	-28.84	-33.14	-66.631	-70.976	-29739.835	-21683.771	-29644.366	-21579.652
M ^P _{ro}	-36.96	-17.71	-73.245	-52.780	-14511.616	-10914.749	-14401.410	-10844.261

Table 8. Comparison of binding affinities of EGCG with reference drugs.

Target	Ligand		
	EGCG	Remdesivir	Ivermectin
Spike	-52.14	-77.56	-
Main protease	-28.84	-45.46	-22.90
ACE-2	-36.96	-37.20	-48.24

inhibit specific antigen presentation, T-cell activation, proliferation and migration into the epithelium, basal keratinocytes apoptosis, signaling pathway activation, MMP-2, and MMP-9 activity, as well increased secretion of RANTES, and can modulate the imbalance seen due to lack of transforming growth factor- beta1 which are implicated in the pathogenesis of OLP [4]. Several researches have proven that EGCG provides numerous help

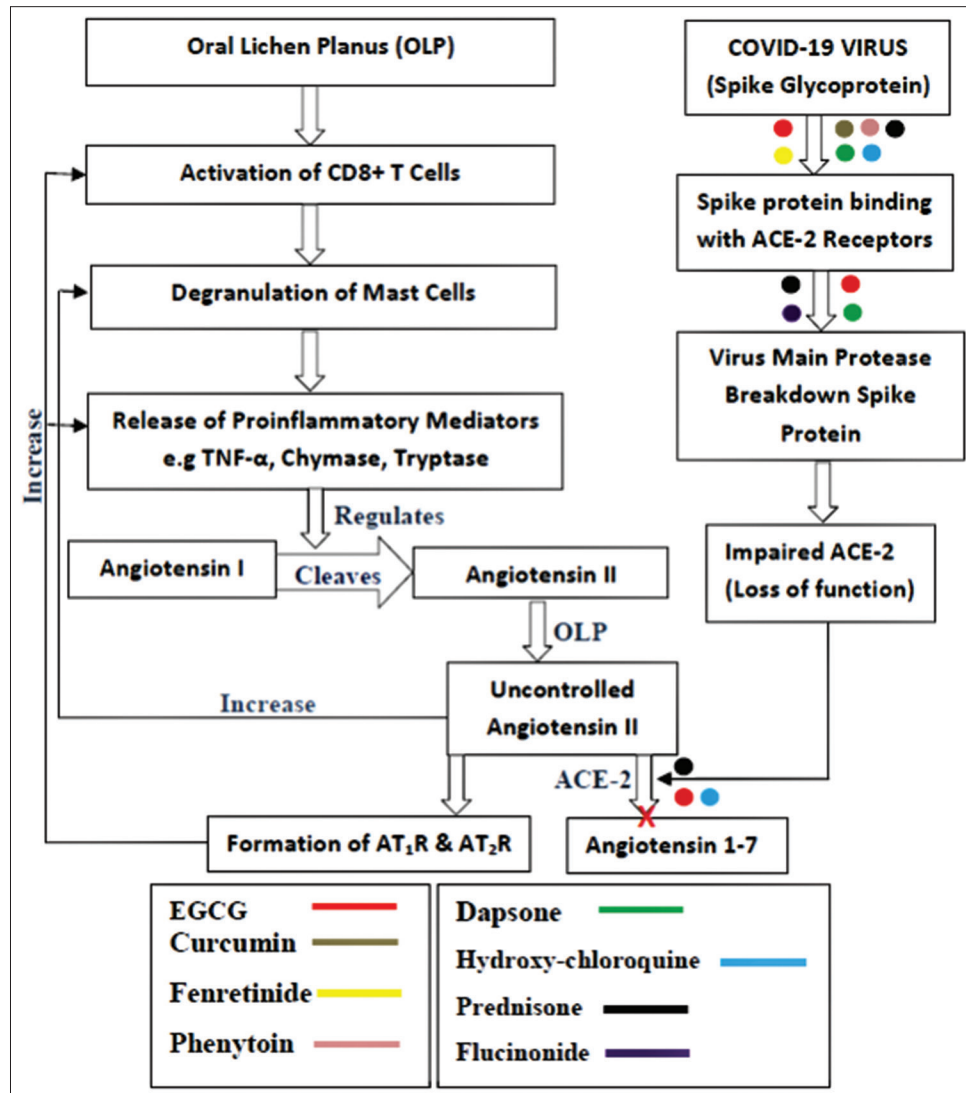


Figure 9. Flowchart depicts the possible interactions between Oral Lichen Planus and COVID-19. Hypothetical analyses of few drugs acting on various target proteins whose MD score is below -3.

in patient suffering from cancer, diabetes, obesity, skin and heart diseases. They are proven to be safe to consume without many side effects. IL-6, TNF- α , and IFNs levels were elevated in SARS-CoV-2 patients in recent studies [22]. As an alternate therapy, EGCG may provide an answer in managing various signs and symptoms related to COVID-19 infection.

Subsequently, in OLP T-cell lymphocyte is activated causing proliferation as well as killing of keratinocyte mediated by CD8+ cytotoxic T- cells [21-23]. Due to T-cell activation, it also involves AT₁R receptors from Angiotensin II. Studies have shown that supplementing EGCG may act as a proteasome inhibitor in concentrations of 2.5–10 μ M both *in-vivo* and *in-vitro* which can decrease T-cell activation and proliferation as well as regulating the migration of cytotoxic CD8+ T cells to sites of inflammation [22,24]. In addition, EGCG can decrease upregulation of endothelial cell adhesion molecule (CD62E, CD54, and CD106) and migratory properties of CD8+ T cells

to sites of inflammation by down regulating CD11b expression on CD8+ T cells [23]. Some studies have shown that EGCG by combining with helper CD4+ T cells stops the virus from entering and binding to the host cells [24,25]. It has been shown to down regulate IL-1 β -induced RANTES [4,5,26].

Follow the loss of function ACE-2 due to binding with SARS-CoV-2 leads to uninhibited Angiotensin II which affects the expression of MMP-2 and MMP-9. A study conducted by Demeule *et al.* shows EGCG which inhibits MMP-2, MMP-9 [27]. It also further suppresses MMP-9 activity and expression. Thus we hypothesized that EGCG is expected to be a best natural alternative therapeutic drug for OLP and COVID-19.

5. Conclusion

With the rapid spread of the COVID-19 pandemic, a race against time had started where the development of drug against SARS-CoV-2 is urgently desired. The main aim of an emergent

drug is to target the M^{pro} (M^{pro} or 3CL^{pro}), Spike Protein S1 of coronavirus and Human ACE-2 with natural compounds which has lesser to no side effect, inexpensive and effective. Therefore, bioinformatic and computational biology are the best virtual method to design and identify chemical structure of potential drugs which in our study is EGCG, a natural compound. EGCG as potential drugs have shown to target proteins responsible for SARS-CoV-2. In total, this research presents a strong indication that EGCG may develop into potent and selective inhibitors of SARS-CoV-2 for the therapeutic management of COVID-19 after required clinical validations.

Acknowledgments

The authors are thankful to the Department of Applied Sciences, Indian Institute of Information Technology, Allahabad for providing us the facilities and encouragements.

Conflict of Interest

The authors declare no conflict of interest.

References

- [1] Ritchie H, Mathieu E, Rodés-Guirao L, Appel C, Giattino C, Ortiz-Ospina E, *et al.* Coronavirus Pandemic (COVID-19); 2020. Available from: <https://ourworldindata.org/coronavirus> [Last accessed on 2021 Dec 24].
- [2] Dhama K, Khan S, Tiwari R, Sircar S, Bhat S, Malik YS, *et al.* Coronavirus Disease 2019-COVID-19. Clin Microbiol Rev 2020;33:e00028.
- [3] Jairajpuri DS, Hussain A, Nasreen K, Mohammad T, Anjum F, Rehman MT, *et al.* Identification of Natural Compounds as Potent Inhibitors of SARS-CoV-2 Main Protease Using Combined Docking and Molecular Dynamics Simulations. Saudi J Biol Sci 2021;28:2423-31.
- [4] Zhang J, Zhou G. Green tea Consumption: An Alternative Approach to Managing Oral Lichen Planus. Inflamm Res 2012;61:535-9.
- [5] Pratyush S, Pratik P, Raghu AR, Ankur KS, Monica S. Current Assessments Regarding the Pathogenesis and Treatment Strategies of Oral Lichen Planus a Review. Asian Pac J Health Sci 2014;1:96-103.
- [6] Gheblawi M, Wang K, Viveiros A, Nguyen Q, Zhong JC, Turner AJ, *et al.* Angiotensin-Converting Enzyme 2: SARS-CoV-2 Receptor and Regulator of the Renin-Angiotensin System. Circ Res 2020;126:1456-74.
- [7] Donoghue M, Hsieh F, Baronas E, Godbout K, Gosselin M, Stagliano N, *et al.* A Novel Angiotensin-converting Enzyme-related Carboxypeptidase (ACE-2) Converts Angiotensin I to Angiotensin 1-9. Circ Res 2000;87:E1-9.
- [8] Wang K, Gheblawi M, Oudit GY. Angiotensin Converting Enzyme 2: A Double-Edged Sword. Circulation. 2020;142:426-8.
- [9] Kuan TC, Chen MY, Liao YC, Ko L, Hong YH, Yen CY, *et al.* Angiotensin II Downregulates ACE-2 Mediated Enhancement of MMP-2 Activity in Human Cardiofibroblasts. Biochem Cell Biol 2013;91:435-42.
- [10] Steagall WK, Stylianou M, Pacheco-Rodriguez G, Moss J. Angiotensin-Converting Enzyme Inhibitors May Affect Pulmonary Function in Lymphangioleiomyomatosis. JCI Insight 2019;4:e126703.
- [11] Sastry GM, Adzhigirey M, Day T, Annabhimoju R, Sherman W. Protein and Ligand Preparation: Parameters, Protocols, and Influence on Virtual Screening Enrichments. J Comput Aided Mol Des 2013;27:221-34.
- [12] Halgren TA. Identifying and Characterizing Binding Sites and Assessing Druggability. J Chem Inf Mod 2009;49:377-38.
- [13] Friesner RA, Murphy RB, Repasky MP, Frye LL, Greenwood JR, Halgren TA, *et al.* Extra Precision Glide: Docking and Scoring Incorporating a Model of Hydrophobic Enclosure for Protein-ligand Complexes. J Med Chem 2006;49:6177-96.
- [14] Chakraborty C, Sharma AR, Mallick B, Bhattacharya M, Sharma G, Lee SS. Evaluation of Molecular Interaction, Physicochemical Parameters and Conserved Pattern of SARS-CoV-2 Spike RBD and hACE-2: *In silico* and Molecular Dynamics Approach. Eur Rev Med Pharmacol Sci 2021;25:1708-23.
- [15] Almeida-Neto FW, Matos MG, Marinho EM, Marinho MM, de Menezes RR, Sampaio TL, *et al.* *In silico* Study of the Potential Interactions of 4'-Acetamidochalcones with Protein Targets in SARS-CoV-2. Biochem Biophys Res Commun 2021;537:71-7.
- [16] Liang J, Pitsillou E, Karagiannis C, Darmawan KK, Ng K, Hung A, *et al.* Interaction of the Prototypical α -ketoamide Inhibitor with the SARS-CoV-2 Main Protease Active Site *in silico*: Molecular Dynamic Simulations Highlight the Stability of the Ligand-protein Complex. Comput Biol Chem 2020;2020:107292.
- [17] Hirshman SP, Whitson JC. Steepest-descent Moment Method for Three-dimensional Magnetohydrodynamic Equilibria. Phys Fluids 1983;26:3553-68.
- [18] Hess B, Bekker H, Berendsen HJ, Fraaije JG. LINCS: A Linear Constraint Solver for Molecular Simulations. J Comput Chem 1997;18:1463-72.
- [19] Cheatham TE, Miller JL, Fox T, Darden TA, Kollman PA. Molecular Dynamics Simulations on Solvated Biomolecular Systems: The Particle Mesh Ewald Method Leads to Stable Trajectories of DNA, RNA and Proteins. J Am Chem Soc 1995;117:4193-4.
- [20] Rosa SG, Santos WC. Clinical Trials on Drug Repositioning for COVID-19 Treatment. Rev Panam Salud Publica 2020;44:e40.
- [21] Maurya VK, Kumar S, Prasad AK, Bhatt ML, Saxena SK. Structure-based Drug Designing for Potential Antiviral Activity of Selected Natural Products from Ayurveda against SARS-CoV-2 Spike Glycoprotein and its Cellular

- Receptor. *Virusdisease* 2020;31:179-93.
- [22] Granja A, Frias I, Neves AR, Pinheiro M, Reis S. Therapeutic Potential of Epigallocatechin Gallate Nanodelivery Systems. *Biomed Res Int* 2017;2017:5813793.
- [23] Pae M, Ren Z, Meydani M, Shang F, Meydani SN, Wu D. Epigallocatechin-3-Gallate Directly Suppresses T Cell Proliferation through Impaired IL-2 Utilization and Cell Cycle Progression. *J Nutr* 2010;140:1509-15.
- [24] Berges C, Haberstock H, Fuchs D, Miltz M, Sadeghi M, Opelz G, *et al.* Proteasome Inhibition Suppresses Essential Immune Functions of Human CD4⁺ T Cells. *Immunology* 2008;124:234-46.
- [25] Kawai K, Tsuno NH, Kitayama J, Okaji Y, Yazawa K, Asakage M, *et al.* Epigallocatechin Gallate Attenuates Adhesion and Migration of CD8⁺ T cells by Binding to CD11b. *J Allergy Clin Immunol* 2004;113:1211-7.
- [26] Ho YC, Yang SF, Peng CY, Chou MY, Chang YC. Epigallocatechin-3-gallate Inhibits the Invasion of Human Oral Cancer Cells and Decreases the Productions of Matrix Metalloproteinases and Urokinase-plasminogen Activator. *J Oral Pathol Med* 2007;36:588-93.
- [27] Demeule M, Brossard M, Pagé M, Gingras D, Béliveau R. Matrix Metalloproteinase Inhibition by Green Tea Catechins. *Biochim Biophys Acta* 2000;1478:51-60.

Publisher's note

Whioce Publishing remains neutral with regard to jurisdictional claims in published maps and institutional affiliations.



ORIGINAL ARTICLE

Lichen planus drugs re-purposing as potential anti COVID-19 therapeutics through molecular docking and molecular dynamics simulation approach

Supplementary data

1. The protein structures selected for the docking studies are shown in [figures 1, 2, and 3](#) for spike protein, ACE-2, and Mpro, respectively.



Figure 1. Spike glycoprotein (PDB ID: 6VYB) structure.

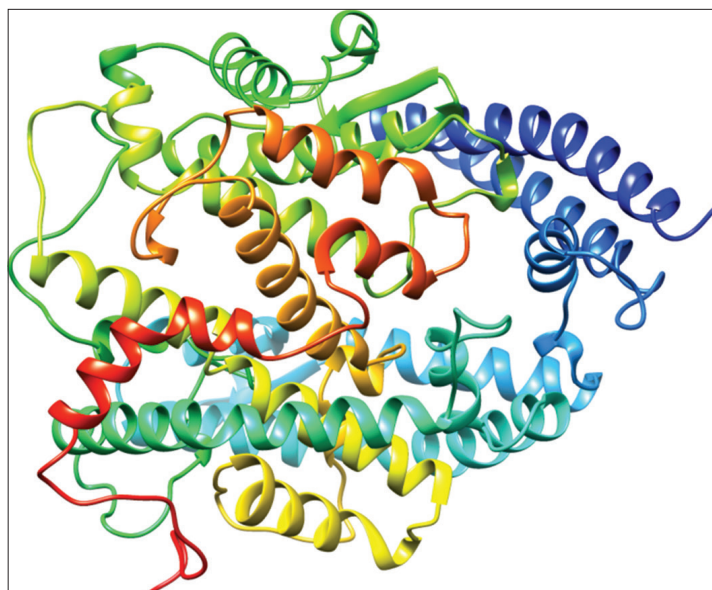


Figure 2. Human ACE-2 (PDB ID: 1R42) structure.

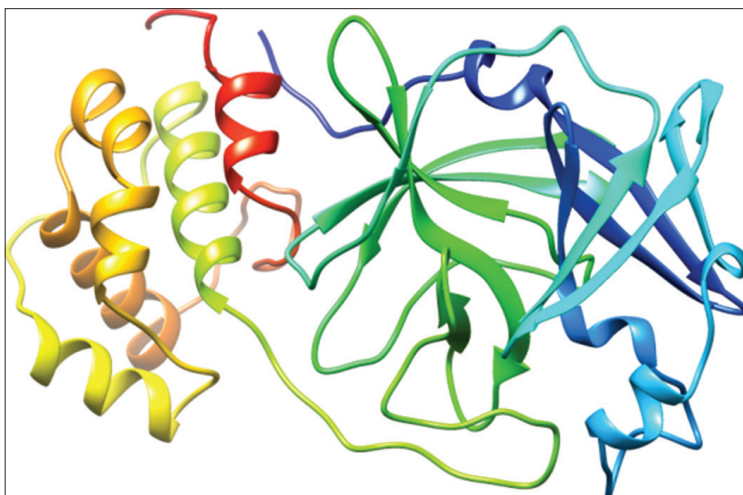


Figure 3. Main protease (PDB ID: 6LU7) structure.

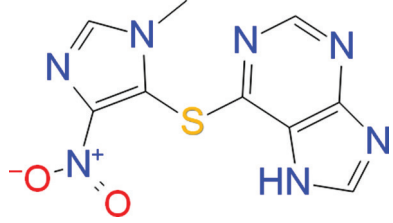
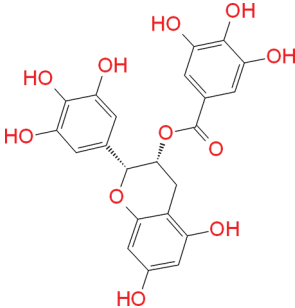
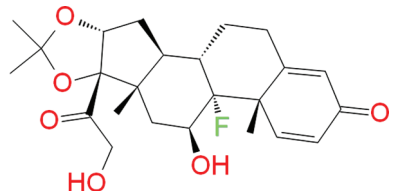
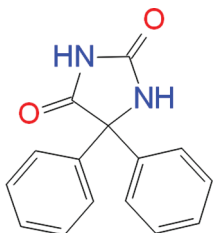
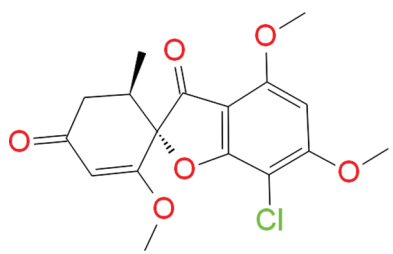
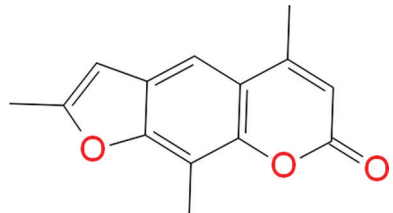
2. The structures of selected ligands along with their PubChem IDs are as shown in Table 1.

Table 1. Chemical structures of the selected drugs with their PubChem ID.

No.	Drugs used against OLP	PubChem ID	Structures
1.	Hydroxy-chloroquine	3652	
2.	Prednisone	5865	
3.	Dapsone	2955	
4.	Flucanionide	9642	
5.	Curcumin	969516	

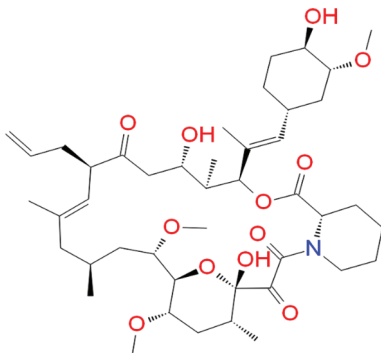
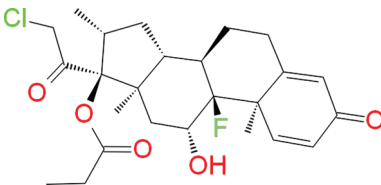
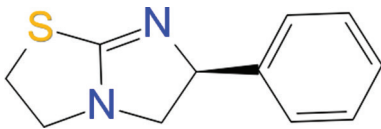
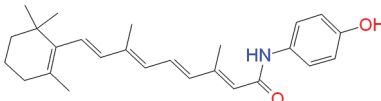
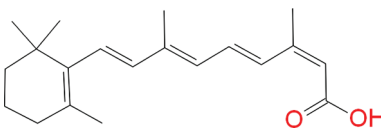
(Contd...)

Table 1. (Continued).

No.	Drugs used against OLP	PubChem ID	Structures
6.	Azathioprine	2265	
7.	Epigallocatechin-3-gallate	65064	
8.	Triamcinolone acetonide	6436	
9.	Phenytoin	1775	
10.	Griseofulvin	441140	
11.	Trioxsalen	5585	

(Contd...)

Table 1. (Continued).

No.	Drugs used against OLP	PubChem ID	Structures
12.	Tacrolimus	445643	
13.	Clobetasol propionate	32798	
14.	Levamisole	26879	
15.	Fenretinide	5288209	
16.	Isotretinoin	5282379	

3. Docking result of co-crystallized ligand for Mpro.

We found inhibitor N-[(5-METHYLISOXAZOL-3-YL) CARBONYL] ALANYL-L-VALYL-N~1~((1R,2Z)-4-(BENZYLOXY)-4-OXO-1-[[[(3R)-2-OXOPYRROLIDIN-3-YL] METHYL} BUT-2-ENYL)-L-LEUCINAMIDE in structure 6LU7 (main protease), after docking of this ligand with respective enzyme, the docking score was found to be lower (-3.996) than the predicted potential drug against COVID-19 for main-protease (-5.020). Its docking result and interaction diagram is as shown in Table 2.

Here in the interaction diagram shown in Table 2, it can be observed that, interacting amino acids are SER 139 forming H-bond, TYR 126 forming Pi-Pi stacking, SER 284, and LYS 5 forming H-bonds through water bridge.

4. Curcumin (-4.746) and Fenretide (-4.417) have also shown significant docking results against spike protein along with EGCG. Their docking values are given in the manuscript (Table 3) while their interaction diagrams are presented as shown in Figures 4 and 5 respectively.

For curcumin, interacting amino acids are PHE 342 and ALA 344 forming Pi-Pi stacking and H-bond, respectively as shown in Figure 4.

5. Along with EGCG, Prednisone has shown considerable docking interaction with all selected targets, that is, with spike (-3.322), ACE-2 (-3.474), and Mpro (-4.439). Its interaction diagrams with all targets are as shown in Figures 6-8.

While for fenretide, interacting amino acids are PHE 342 forming Pi-Pi stacking as depicted in Figure 5.

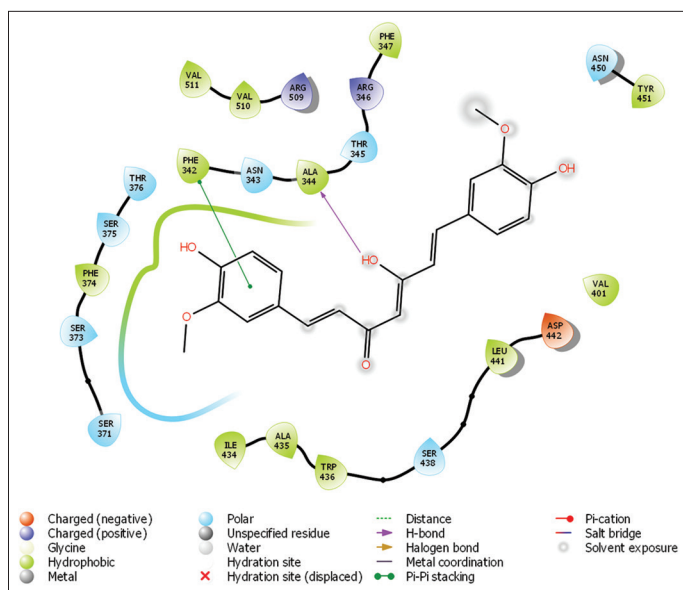
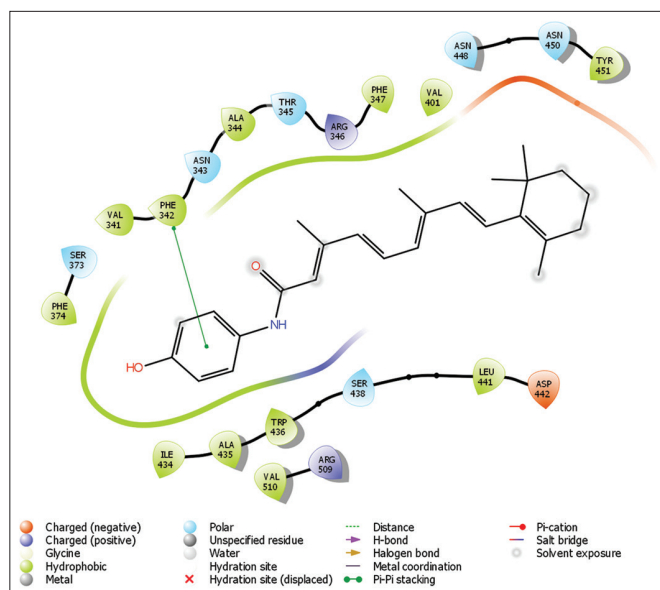
Here for prednisone, interacting amino acids are ALA 344 forming H-bond with spike protein shown clearly in Figure 6.

Here, interacting amino acids are GLN 127 and LYS 5 forming H-bonds through water-bridge, LYS 137, and GLU 290 forming H-bonds, which can be noticed the strong interaction between prednisone and main-protease as shown in Figure 7.

Here in the interaction of prednisone with human ACE-2, interacting amino acids are ALA 387 forming H-bond and GLU 37 forming H-bond through water-bridge as shown in Figure 8.

Table 2. Docking result of co-crystallized ligand for Mpro.

Ligand	Docking score	Interaction Diagram
N-[(5-METHYLISOXAZOL-3-YL) CARBONYL] ALANYL-L-VALYL-N~1~-((1R,2Z)-4-(BENZYLOXY)-4-OXO-1- -[(3R)-2-OXOPYRROLIDIN-3-YL] METHYL} BUT-2-ENYL) -L-LEUCINAMIDE	-3.996	

**Figure 4.** Interaction diagram of curcumin with spike protein.**Figure 5.** Interaction diagram of fenretide with spike protein.

6. Here, we have manually mutated pocket residues of Spike protein for Alpha, Beta, Gamma, delta, and Omicron variants and performed their docking with tested compounds using the software Maestro 12.6. We have observed the highest docking values with the Epigallocatechin-3-gallate for all above mentioned variants of S-protein, their docking result is as shown in Table 3.

Interaction images of proposed drug EGCG with all variants of spike protein is as shown in Figures 9-13, which are alpha, beta, gamma, delta and omicron variants respectively.

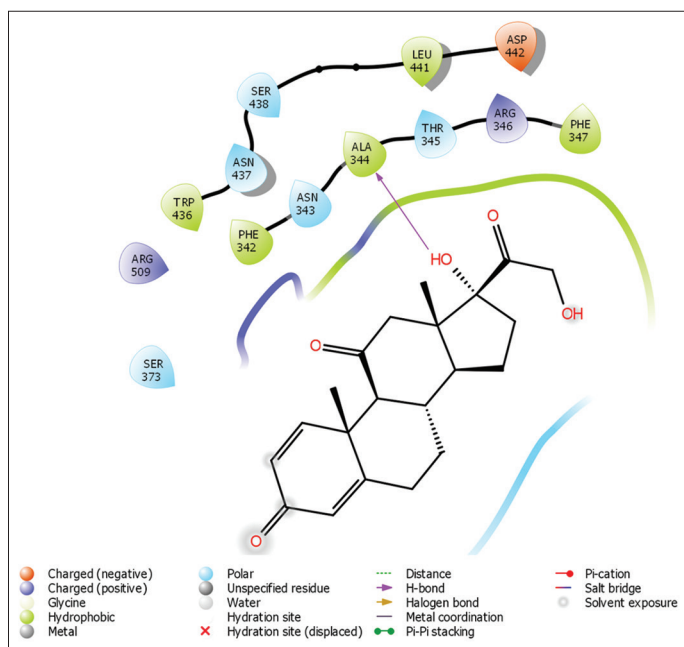


Figure 6. Interaction diagram of prednisone with spike protein.

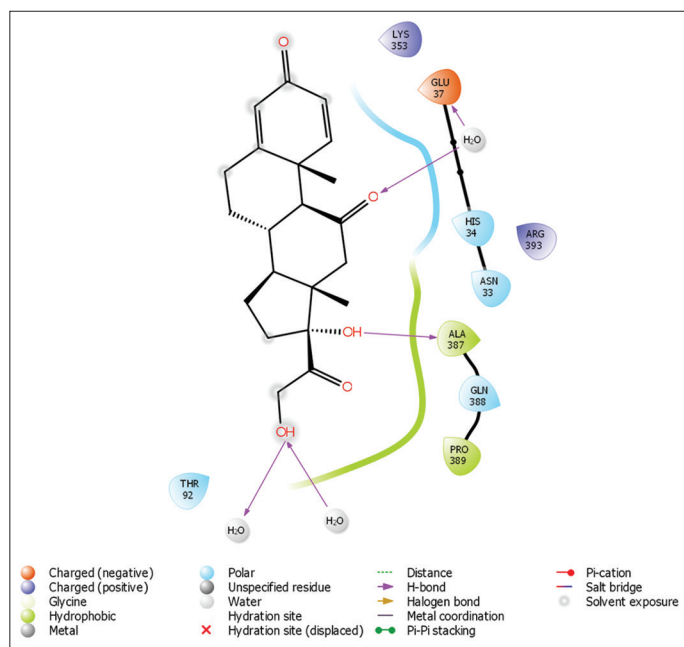


Figure 8. Interaction diagram of prednisone with ACE-2.

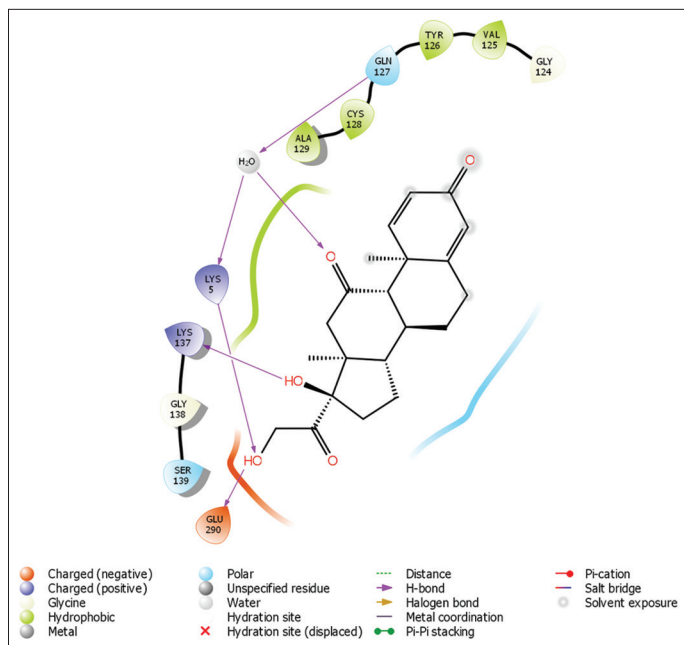


Figure 7. Interaction diagram of prednisone with Mpro.

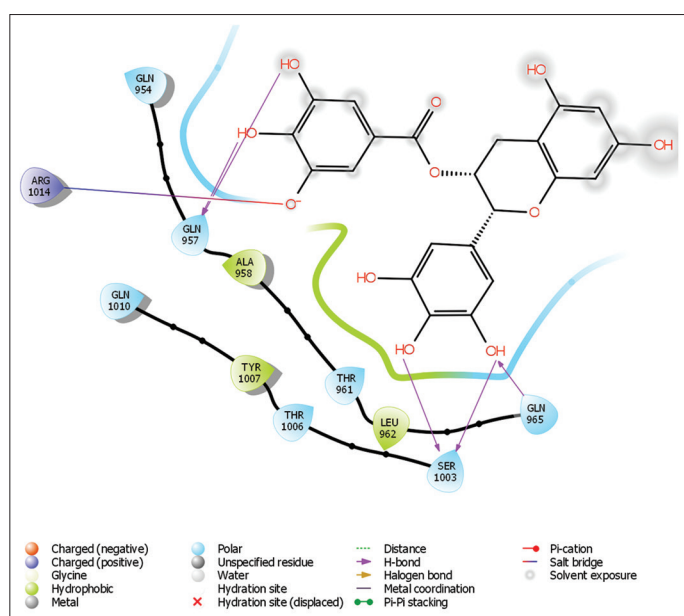


Figure 9. Interaction image of EGCG with alpha variant of spike protein.

Table 3. Detailed docking result of EGCG with variants of S-protein.

Variants	Docking score	Glide gscore	Glide emodel	Interaction residues	Interaction type
Alpha	-4.119	-5.968	-49.484	GLN 957, GLN 965, SER 1003, ARG 1014	Five H-bonds, One salt bridge
Beta	-4.072	-5.921	-46.070	CYX 379, LYS 378, ARG 408, PRO 412	Six H-bonds
Gamma	-4.132	-4.390	-43.556	GLY 381, SER 383, PHE 429	Five H-bonds
Delta	-3.941	-5.790	-50.858	ASP 389, LYS 528, GLY 545	Six H-bonds, One Salt bridge, One Pi-cation
Omicron	-6.532	-6.610	-43.805	SER 383, CYS 379, PHE 377	Six H-bonds

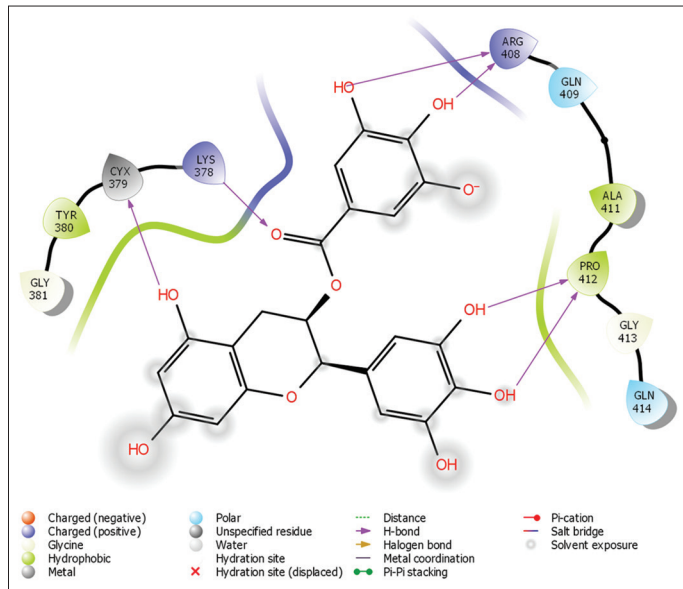


Figure 10. Interaction image of EGCG with beta variant of spike protein.

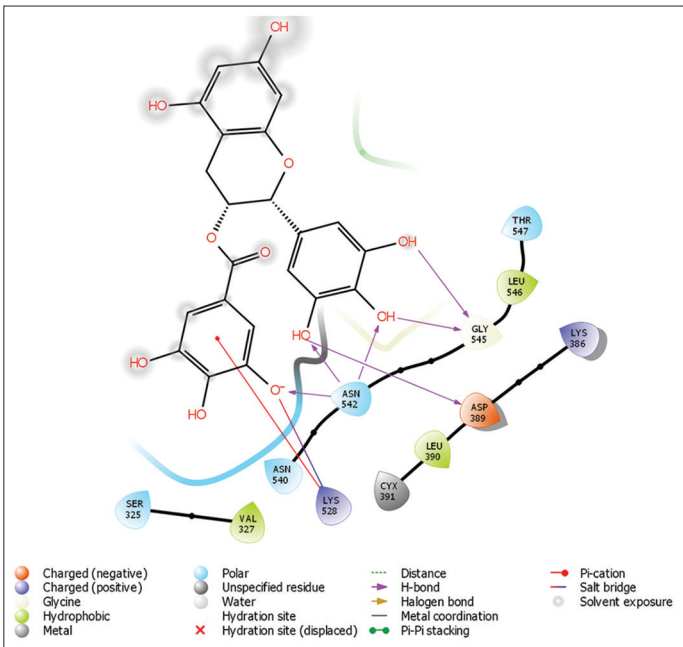


Figure 12. Interaction image of EGCG with delta variant of spike protein.

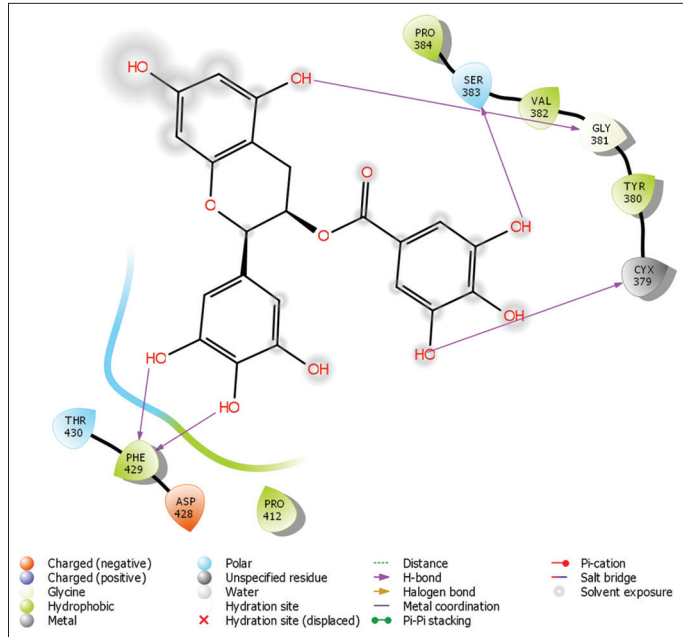


Figure 11. Interaction image of EGCG with gamma variant of spike protein.

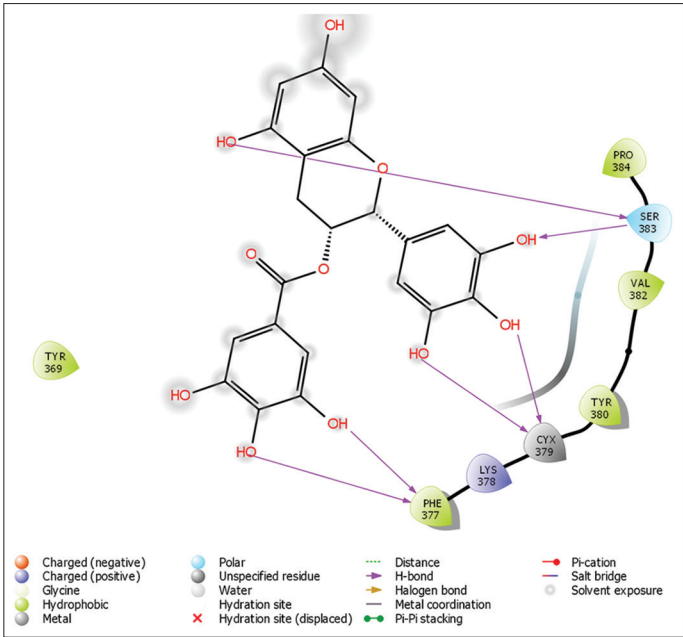


Figure 13. Interaction image of EGCG with omicron variant of spike protein.